Eur Phys J C **39**, s3, s1–s5 (2004)
Digital Object Identifier (DOI) 10.1140/epjcd/s2004-01-008-8

EPJ C direct
electronic only

Young Scientists:

Measurement of the proton structure function F_2 in QED Compton scattering at HERA

V. Lendermann

Deutsches Elektronen-Synchrotron (DESY), Notkestr. 85, D-22607 Hamburg, Germany; e-mail: victor@mail.desy.de

Received: 14 November 2003 / Accepted: 18 February 2004 /
Published online: 5 April 2004 –

Abstract. QED Compton scattering at HERA is proposed for a measurement of the proton structure function F_2 at low momentum transfers Q^2. It is shown that the analysis of inelastic QED Compton events allows the extension of present HERA structure function measurements to a kinematic domain, which up to now was only accessed in fixed target data. Preliminary results of such a measurement performed by the H1 Collaboration are presented. The results are in good agreement with the measurements from fixed target experiments wherever they overlap.

1 Introduction

Measurements of deep inelastic lepton-proton scattering (DIS) provide information which is crucial to our understanding of proton structure and which has played a decisive role in the development of the theory of strong interactions, Quantum Chromodynamics (QCD). Since the discovery of Bjorken scaling [1] and its violation [2,3] at fixed target experiments, much progress has been made in extending the kinematic range of measurements in terms of the Bjorken variable x and the negative four-momentum transfer squared Q^2. In particular, the H1 and ZEUS experiments, running since 1992 at the HERA ep collider, have shown that the Q^2 evolution of the proton structure function $F_2(x, Q^2)$ is well described by perturbative QCD throughout a wide range in x and Q^2 [4, 5, 6, 7]. However, at small Q^2 deviations from pQCD predictions are observed [7,8], indicating the transition into a regime in which non-perturbative effects dominate and the data can only be described by phenomenological models such as those derived from the Regge approach [9].

In order to study this non-perturbative regime, the structure function F_2 has been measured at very low values of Q^2, which are accessible at HERA via special devices mounted close to the outgoing electron beam direction [8], thus facilitating measurements of the scattered electron at very low angles. These devices, however, do not cover the transition region around $Q^2 \sim 1\,\mathrm{GeV}^2$, which up to now has only been investigated using "shifted vertex" [10, 11] and Initial State Radiation [12, 13] data. In this article a new approach for an F_2 measurement in the low Q^2 domain is discussed, which utilises ep data with wide angle hard photon radiation, so called QED Compton events. First results of such a measurement performed by the H1 Collaboration are presented.

2 QED Compton scattering

Radiative processes in ep scattering, as depicted in Fig. 1, may be split into three different classes [14,15] with (i) the bremsstrahlung or Bethe-Heitler process corresponding to small virtualities of both the exchanged electron and the exchanged photon, (ii) the QED Compton (QEDC) process with a low exchanged photon and a large exchanged electron virtuality and finally (iii) the radiative DIS process where the photon is collinear either with the incoming (Initial State Radiation, ISR) or the outgoing (Final State Radiation, FSR) electron. All three classes correspond to distinct experimental signatures. For the QEDC scattering process the final state topology is given by an azimuthal back-to-back configuration of the outgoing electron and photon detected under rather large scattering angles. In this configuration their transverse momenta balance such

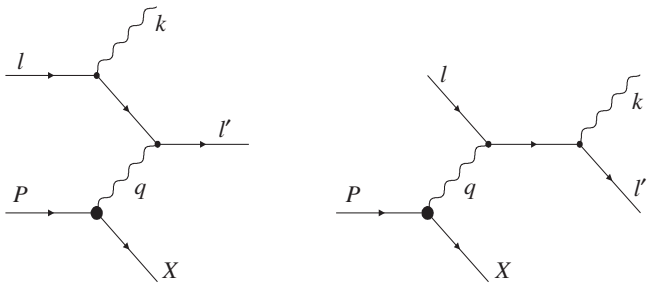

Fig. 1. Lowest order Feynman diagrams for the radiative process $ep \to e\gamma X$ with photon emission from the electron line. l, P represent the four-momenta of the incoming electron and the incoming proton, while l', k and X are the four-momenta of the scattered electron, the radiated photon and the hadronic final state, respectively

that very low values of the exchanged photon virtuality Q^2 are experimentally accessible.

To correctly describe the process $ep \to e\gamma X$ the standard kinematic variables x and Q^2, used to describe inclusive deep inelastic scattering, have to be redefined in order to account for the additional photon in the final state

$$Q^2 = -q^2 = -(l - l' - k)^2 \ , \qquad x = \frac{Q^2}{2P \cdot (l - l' - k)} \ . \tag{1}$$

Here l and P are the four-momenta of the incoming electron and the incoming proton, and l' and k represent the momenta of the scattered electron and the radiated photon, respectively (Fig. 1), and $s = (l+P)^2$ is the ep centre-of-mass energy squared. On the other hand, the definitions remain unchanged if these variables are calculated using the four-momentum of the hadronic final state, X:

$$Q^2 = -q^2 = -(X - P)^2 \ , \qquad x = \frac{Q^2}{2P \cdot (X - P)} \ . \tag{2}$$

Three further non-trivial degrees of freedom have to be taken into account for a full description of the differential QEDC scattering cross section. In the formalism presented in [14] the Lorentz invariant scale variable $x_\gamma = (q \cdot l)/(P \cdot l)$ and the scattering solid angle Ω^* defined in the centre-of-mass frame of the virtual Compton process and encapsulating two degrees of freedom are employed for this purpose. The cross section is then given by [14]

$$\frac{d^4\sigma^{ep\to e\gamma X}}{dx dx_\gamma dQ^2 d\Omega^*} = f^T_{\gamma^*/p}(x, x_\gamma, Q^2) \left[\frac{d\sigma}{d\Omega^*}\right]^T + f^L_{\gamma^*/p}(x, x_\gamma, Q^2) \left[\frac{d\sigma}{d\Omega^*}\right]^L , \tag{3}$$

where $[d\sigma/d\Omega^*]^{T,L}$ are the differential cross sections of the process $e\gamma^* \to e\gamma$ for transverse and longitudinal polarised photons, fully calculable in the framework of QED [14], and $f^{T,L}_{\gamma^*/p}$ represent the corresponding virtual photon spectra, which may be expressed in terms of the photo-absorption cross sections $\sigma^{T,L}_{\gamma^* p}$. Depending on the value of the invariant mass of the hadronic final state, $W = [Q^2(1-x)/x + m_p^2]^{\frac{1}{2}}$, one has to consider three separate contributions, in order to specify $\sigma^{T,L}_{\gamma^* p}$:

1. Elastic scattering, for which the proton stays intact ($W = m_p$, $x = 1$). This channel is well measured, and the cross section is given by the electric and magnetic form factors G_E and G_M;
2. Resonance production, where the total mass of the hadronic final state X lies in the range $m_p + m_\pi \lesssim W \lesssim 2\,\mathrm{GeV}$;
3. Continuum inelastic scattering at $W \gtrsim 2\,\mathrm{GeV}$. In this region the $\gamma^* p$ cross section is defined through the structure functions F_2 and F_L.

It is proposed in [16], to employ the latter contribution for a measurement of F_2.

3 Experimental technique

The H1 measurement is performed on $9.25\,\mathrm{pb}^{-1}$ of e^+p data with centre-of-mass energy $\sqrt{s} = 301\,\mathrm{GeV}$, which were collected at HERA in 1997.

The outgoing electron and photon in QEDC events are selected in the H1 detector [17] by requiring two energy depositions (clusters) in the electromagnetic part of the backward[1] lead-fibre calorimeter SpaCal [18]. The Backward Drift Chamber (BDC) [19] situated in front of the SpaCal is employed as a pre-shower detector to increase the precision of the cluster position measurement for electrons and converted photons. In events with the electron scattered in the inner part of the SpaCal, the Backward Silicon Tracker (BST) [20] is used to measure the electron polar angle and to reconstruct the interaction vertex position. In events in which the electron is scattered out of the BST acceptance, the Central Inner Proportional Chamber (CIP) [17] is employed in conjunction with BDC and SpaCal to determine the vertex coordinates. The hadronic final state is measured in the Liquid Argon Calorimeter (LAr) [17].

4 Event simulation

The cross section expression (3) is implemented in the COMPTON Monte Carlo event generator [14, 21]. The program also calculates higher order corrections for Initial State Radiation in the peaking approximation [22,23]. However, as this generator was primarily written for use in analyses of elastic QEDC events, in the original version a rather crude approach is employed to describe the resonance region and only simple scale invariant F_2 parameterisations are used to model the continuum inelastic domain. Furthermore, no hadronisation of the final state X is performed.

For the investigation of inelastic QEDC events a new version of the COMPTON generator was developed [24] which includes detailed parameterisations for the resonance [25] and the continuum [26] regions. In addition, several packages for a complete simulation of the hadronic final state have been interfaced to the program. For the present study the SOPHIA package [27] is used in the range of low Q^2 ($Q^2 < 2\,\mathrm{GeV}$) or low masses of the hadronic final state ($W < 5\,\mathrm{GeV}$), while the Quark Parton Model with subsequent Lund string fragmentation [28] is employed at higher W and higher Q^2.

The SOPHIA model provides a minimum bias description of photoproduction processes reproducing a large set of available data. The simulation includes production of major baryon resonances, direct pion production, multiparticle production based on the Dual Parton Model [29] with subsequent Lund string fragmentation, as well as the diffractive production of light vector mesons.

[1] The z axis of the right-handed coordinate system used by H1 is defined to lie along the direction of the incident proton beam and the origin to be at the nominal ep interaction vertex. The backward direction is thus defined through $z < 0$

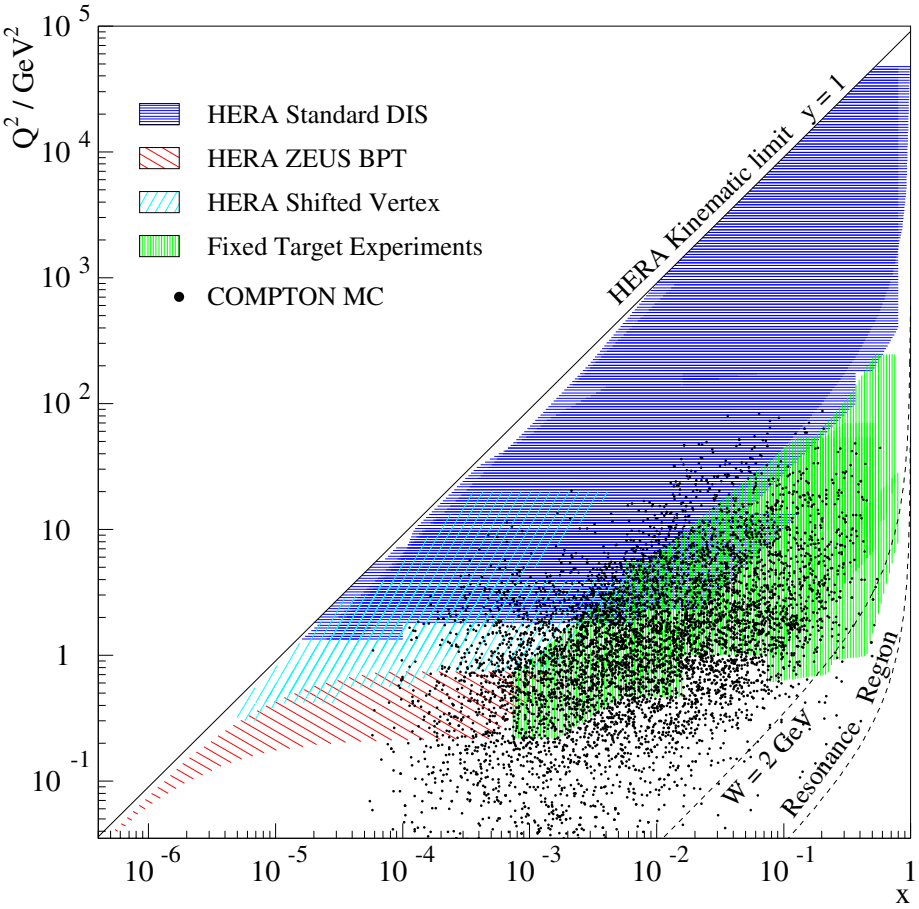

Fig. 2. Kinematic domain of inelastic QED Compton events in comparison to the regions covered by inclusive DIS measurements at HERA and fixed target experiments

5 Background processes

A prominent background to inelastic QEDC scattering arises from inclusive DIS events in which one particle from the hadronic final state (typically a π^0) fakes the outgoing photon, producing a cluster in the electromagnetic SpaCal. Such events are modelled using the DJANGO MC generator [30]. At high $y = Q^2/xs$, where the hadronic final state lies mostly in the hemisphere of the scattered electron and photon, this process dominates the QEDC signal, hampering a clean QEDC event selection.

Another source of significant background is Deeply Virtual Compton Scattering (DVCS), in which the final state photon is produced in the virtual photon proton collision. DVCS and QEDC are indistinguishable experimentally, and differ only in the kinematic distributions of the outgoing electron and photon. Nevertheless, both processes can be simulated separately, as the interference between them does not influence the energy and polar angle distributions of the final state particles in the leading twist approximation. Elastic DVCS events were simulated by the TINTIN generator [31] and the cross section was normalised to the H1 results [32]. At present there is neither a theoretical prediction, nor a measurement for the inelastic DVCS cross section. The ratio of the inelastic to elastic scattering cross section was therefore estimated experimentally to be of a similar size to that for diffractive vector meson electroproduction.

Further background sources considered are comparatively small.

6 Details of the measurement

The phase space covered by a QEDC MC sample after the experimental event selection is shown in Fig. 2. Compared to the kinematic range accessed at HERA via standard deep inelastic scattering, the QEDC events clearly extend to lower Q^2. For inclusive DIS the outgoing electron is not detected for such low values of Q^2 as it is scattered at small angles, escaping unseen through the beam pipe. QEDC events, however, with the electron and photon in the final state balancing in transverse momentum, reach into the transition region below $Q^2 < 1.5\,\mathrm{GeV}^2$, which otherwise is only accessed through ISR [12,13] (not shown), shifted vertex [11,10] and BPT [8] data. However, these latter data do not extend the low Q^2 F_2 measurements to such high x as QEDC events. It is therefore the range of medium to high x which is of special interest when analysing QEDC scattering.

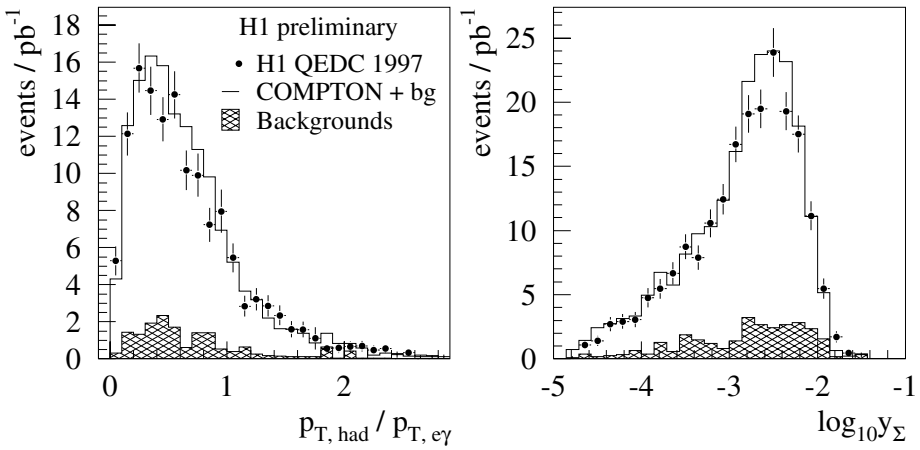

Fig. 3. a Ratio of the total measured transverse momentum of hadrons to the total transverse momentum of the $e\gamma$ system; **b** y_Σ distribution. H1 data are depicted by the closed circles. The solid histogram represents the sum of COMPTON MC events with all background contributions added. The hatched histogram denotes the sum of all background contributions

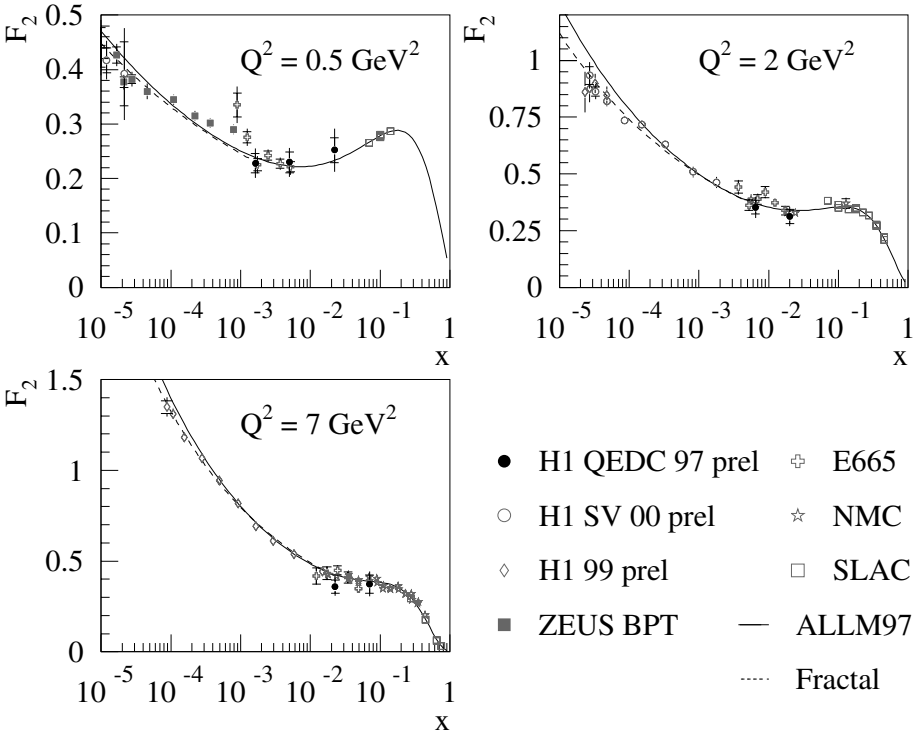

Fig. 4. Preliminary results of an F_2 measurement in QED Compton scattering by H1 (*closed circles*), compared with other measurements at HERA (*closed squares* [8], *open diamonds* [34] and *open circles* [35]) and fixed target experiments (*open squares* [36], *open stars* [37] and *open crosses* [38]). The *solid line* depicts the ALLM97 parameterisation [26], while the *dashed line* represents a 'Fractal' fit [39], which is plotted in the range $y > 0.003$

In QEDC events at HERA the kinematic variables Q^2, x and y can be reconstructed using the parameters of the outgoing electron and photon or those of the hadronic final state. However, for the kinematic range in question, the variables x and y cannot be determined solely from the measured electron and photon four-momenta, since the resolution deteriorates as $1/y$. Therefore, these variables are reconstructed using the so-called Sigma method [33] which employs both hadrons as well as the electron and the photon. As low y corresponds to low scattering angles of the final state hadrons, one of the main challenges for the analysis is a good understanding of the hadronic energy flow and the acceptance corrections in the forward region of the detector. This requires a good modelling of hadronisation processes at low invariant masses W, for which the SOPHIA package (see Sect. 4) is employed in this analysis.

The quality of the description of the hadronic final state, comprising both the hadron distribution modelled by the SOPHIA package and the subsequent simulation of the detector response, is illustrated in Fig. 3a, in which the ratio of the total transverse momentum of measured hadrons $p_{t,\mathrm{had}}$ to the total transverse momentum of the $e\gamma$ system $p_{t,e\gamma}$ is plotted. The simulation provides a very good description of data. Due to losses in the very forward region, outside the acceptance of the LAr calorimeter, the distribution peaks at values smaller than one. One should note, however, that for the calculation of the kinematic variables y and x with the Sigma method, the total $E-p_z$ of hadrons is used, which is much less sensitive to the losses in the beam pipe than the transverse momentum.

The event distribution in y shown in Fig. 3b demonstrates the good quality of both the hadronic simulation and the cross section description given by the COMPTON program down to the lowest y values, even beyond the range used for the measurement.

7 First results of the H1 measurement

The preliminary F_2 values measured in QED Compton scattering by H1 are shown in Fig. 4 as a function of x at fixed Q^2 and compared to other HERA [34, 35, 8] and fixed target [36, 37, 38] data. Both the statistical and the systematic errors of the H1 measurement lie in the range $8-13\%$ such that the total error lies between 12% and 18%.

The present analysis extends the kinematic range of HERA at very low Q^2 towards higher x values, thus complementing standard inclusive and shifted vertex measurements. The region covered mostly overlaps with the domain of fixed target experiments. A good agreement with their results is observed.

References

1. E.D. Bloom et al. [SLAC–MIT collaboration]: Phys. Rev. Lett. **23**, 930 (1969)
2. D.J. Fox et al.: Phys. Rev. Lett. **33**, 1504 (1974)
3. J.G. de Groot et al.: Z. Phys. C **1**, 143 (1979)
4. C. Adloff et al. [H1 Collaboration]: Eur. Phys. J. C **21**, 33 (2001)
5. C. Adloff et al. [H1 Collaboration]: Eur. Phys. J. C **30**, 1 (2003)
6. S. Chekanov et al. [ZEUS Collaboration]: Eur. Phys. J. C **21**, 443 (2001)
7. C. Adloff et al. [H1 Collaboration]: Phys. Lett. B **393**, 452 (1997)
8. J. Breitweg et al. [ZEUS Collaboration]: Phys. Lett. B **487**, 53 (2000)
9. P.D. Collins: *An Introduction To Regge Theory And High-Energy Physics* (Cambridge, 1977), 445p
10. M. Derrick et al. [ZEUS Collaboration]: Z. Phys. C **69**, 607 (1996)
11. C. Adloff et al. [H1 Collaboration]: Nucl. Phys. B **497**, 3 (1997)
12. ZEUS Collaboration: contributed paper to International Conference on High Energy Physics, ICHEP 2002, Amsterdam, abstract **771**
13. H1 Collaboration: contributed paper to International Conference on High Energy Physics, ICHEP 2002, Amsterdam, abstract **976**
14. A. Courau, P. Kessler: Phys. Rev. D **46**, 117 (1992)
15. T. Ahmed et al. [H1 Collaboration]: Z. Phys. C **66**, 529 (1995)
16. V. Lendermann, H.-C. Schultz-Coulon, D. Wegener: V. Lendermann, H. C. Schultz-Coulon and D. Wegener: Eur. Phys. J. C **31**, 343 (2003), DESY–03–085, hep–ph/0307116
17. I. Abt et al. [H1 Collaboration]: Nucl. Instrum. Meth. A **386**, 310 and 348 (1997)
18. R.D. Appuhn et al. [H1 SpaCal Group]: Nucl. Instrum. Meth. A **374**, 149 (1996), A **382**, 395 (1996), and A **386**, 397 (1997)
19. B. Schwab: Doctoral Thesis, Ruprecht Karl University of Heidelberg, 1996
20. W. Eick et al.: Nucl. Instrum. Meth. A **386**, 81 (1997)
21. T. Carli, A. Courau, S. Kermiche, P. Kessler: in **Proceedings of the Workshop "Physics at HERA", Hamburg, 1991**, DESY, 1992, Vol. 2, p. 902 and Vol. 3, p. 1468
22. E. Etim, G. Pancheri, B. Touschek: Nuovo Cim. B **51S10**, 276 (1967)
23. G. Pancheri: Nuovo Cim. B **60S10**, 321 (1969)
24. V. Lendermann: Doctoral Thesis, University of Dortmund, 2002
25. F.W. Brasse et al.: Nucl. Phys. B **110**, 413 (1976)
26. H. Abramowicz, A. Levy: DESY–97–251, hep–ph/9712415
27. A. Mücke et al.: Comput. Phys. Commun. **124**, 290 (2000)
28. T. Sjöstrand et al.: Comput. Phys. Commun. **135** 238 (2001)
29. A. Capella, U. Sukhatme, C. Tan, J. Tran Thanh Van: Phys. Rept. **236** 225 (1994)
30. G.A. Schuler, H. Spiesberger: in *Proceedings of the Workshop "Physics at HERA", Hamburg, 1991*, DESY, 1992, Vol. 3, p. 1419
31. R. Stamen: Doctoral Thesis, University of Dortmund, 2001
32. C. Adloff et al. [H1 Collaboration]: Phys. Lett. B **517**, 47 (2001)
33. U. Bassler, G. Bernardi: Nucl. Instrum. Meth. A **361**, 197 (1995)
34. H1 Collaboration: contributed paper to the International Europhysics Conference on High Energy Physics, EPS 2001, Budapest, abstract **799**
35. H1 Collaboration: contributed paper to the International Europhysics Conference on High Energy Physics, EPS 2003, Aachen, abstract **082**
36. L.W. Whitlow et al.: Phys. Lett. B **282** 475 (1992)
37. M. Arneodo et al. [New Muon Collaboration]: Nucl. Phys. B **483**, 3 (1997)
38. M.R. Adams et al. [E665 Collaboration]: Phys. Rev. D **54**, 3006 (1996)
39. T. Laštovička: Eur. Phys. J. C **24**, 529 (2002)